A Novel Resonant Converter Topology for DC-to-DC Power Supply

YAN-FEI LIU, Member, IEEE

PARESH C. SEN, Fellow, IEEE
Queen's University
Canada

A class-E dc-to-dc converter with half-wave controlled current rectifier is proposed. It's output voltage is controlled by the conduction angle of the rectifier switch at constant switching frequency. Zero voltage switching for all the switches can be maintained from full load to no load. Its steady state characteristics are analyzed and the effects of the circuit parameters are studied. Some extensions of the proposed converter are also discussed. The analysis is verified by PSPICE simulation and an experimental prototype.

Manuscript received September 9, 1993; revised May 9 and May 31, 1994.

IEEE Log No. T-AES/31/4/12729.

Authors' current addresses: Y.-F. Liu, Bell Northern Research Ltd., P.O. Box 3511, Station C, Ottawa, Ontario, Canada K1Y 4H7; P. C. Sen, Dept. of Electrical Engineering, Queen's University, Kingston, Ontario, Canada K7L 3N6.

0018-9251/95/$4.00 © 1995 IEEE

I. INTRODUCTION

The size of electronic equipment is shrinking steadily. The size of its power supply has to be reduced as well. For the switching power supply, the effective way to reduce the size is to increase the switching frequency so that the size of the filter capacitor and inductor, as well as the transformer, can be reduced as they occupy a large portion of the overall size.

In the PWM (pulsewidth modulated) converter [1–4], the active switch is turned on and off at controlled instant and the switch voltage and current change almost as a step. Because of the finite switching time, large switch current and switch voltage are present at the same time during switching turn on and turn off interval. The switching loss is, therefore, induced for every switching action. At high switching frequency, the switching loss becomes very large. Furthermore, the existence of the layout inductance and junction capacitance of the semiconductor devices causes the electronic switch to inductively turn off and capacitively turn on. The consequence is that large voltage and current spikes are induced and extra power is lost. High switching loss reduces the efficiency of the switching power supply and also requires larger heat sink for the switches. Therefore, it is not suitable to reduce the size of the PWM switching converter by increasing the switching frequency further.

In the resonant converters [5–8], the current flowing through the switches are quasi-sinusoidal and the switching loss is small because the switches are turned on and/or off at zero voltage and/or zero current. Therefore, high switching frequency is achieved and the size of the switching power supply can be reduced. Among the resonant converters, the class-E converters [8–14], both operated at constant switching frequency and variable switching frequency, offer particular advantages in high frequency operation because of extremely low switching loss and simple topology.

In this work, various topologies based on the class-E converter are at first reviewed and their advantages and disadvantages are addressed in next section. In Section III, a class-E converter topology is proposed by employing the concept of the half-wave controlled current rectifier. This topology retains all the merits of the conventional class-E converter and at the same time, overcomes the disadvantages, namely, variable switching frequency control and limited load variation range for lossless operation. The steady state characteristics of the proposed converter are analyzed and the effects of the various circuit parameters are studied in Section IV. Some extensions of the proposed converter are discussed in Section V. In Section VI, PSPICE simulation is made and experimental prototype is built to verify the feasibility of the new converter and the validity of the analysis. Both the analysis and experiment show that the proposed

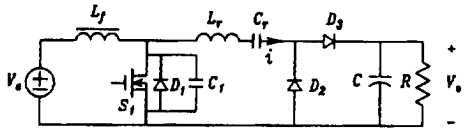

Fig. 1. Class-E dc to dc converter.

topology can maintain the desirable characteristics of zero voltage switching over the entire operating range at constant switching frequency. Section VII is the conclusion.

II. REVIEW OF CLASS-E DC-TO-DC CONVERTERS

The basic class-E dc-to-dc converter [8] is shown in Fig. 1. This topology is suitable for high switching frequency operation because 1) the turn on loss of the metal-oxide-semiconductor field-effect transistor (MOSFET) is zero, 2) the turn off loss is minimized by the parallel capacitor C_1, 3) the body diode of the MOSFET can be utilized, and 4) the parasitic capacitor of the MOSFET can also be included as part of the external capacitor. In addition, the topology configuration is very simple. The dc output voltage is obtained by rectifying the resonant current i. When the load resistor changes, the switching frequency is changed accordingly to regulate the amplitude of the resonant current and hence to maintain the output voltage unchanged. Unfortunately, the switching frequency has to change over a wide range to accommodate the worst combination of the load resistor and supply voltage variation.

Another problem associated with the class-E converter (Fig. 1) is that at small output current, or at large load resistor, the resonant current is unable to discharge the capacitor C_1 completely and zero voltage turn on can not be maintained for S_1. It is shown in [8, 10] that zero voltage turn on can only be maintained for

$$0 < R < R_{\max} \tag{1}$$

where R is the load resistor and the value $R_{\max}$ is dependent on the circuit variables. When load resistor R is larger than $R_{\max}$, zero voltage turn on for S_1 will no longer be present. The circuit cannot operate properly for no load conditions.

Several attempts have been made to solve these problems of the class-E dc-to-dc converter.

In [10], an inductor and a coupling capacitor are added at the input of the rectifier, as shown in Fig. 2. The inductor L_2 is used as impedance inverter so that zero voltage switching can be maintained for larger variation range of the load resistor. The variation range of the switching frequency is also reduced as compared with the conventional class-E converter (Fig. 1). The circuit can operate at no load condition. Unfortunately, there still exists some value of the load resistor at which zero voltage switching for S_1 is lost

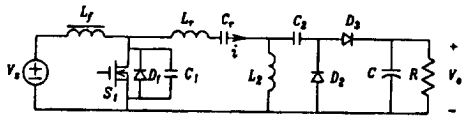

Fig. 2. Class-E converter with inductive impedance inverter.

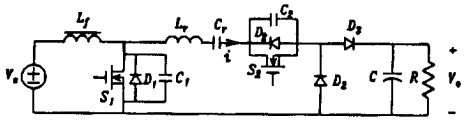

Fig. 3. Class-E converter with switch controlled capacitor.

and the switching frequency has still to vary about 12% to keep the output voltage at a desirable value when load resistor changes.

One limitation of variable switching frequency control is that the filter inductor and filter capacitor have to be designed according to the lowest switching frequency. Another drawback is that the spectrum of the noise generated by the switching converter varies over a wide frequency range. In some circumstances, the switching frequency of the power supply must be kept at certain value to avoid interference with other parts of the electronic equipment. It is, therefore, desirable to keep the switching frequency constant.

Two techniques have been proposed to operate the class-E dc-to-dc converter at the fixed switching frequency [11, 12].

The output voltage of the class-E dc-to-dc converter is dependent on both the switching frequency and the resonant frequency. In [11], a controlled capacitor, called the "switch-controlled capacitor" (SCC), is used to change the equivalent resonant frequency of the resonant branch in the class-E dc-to-dc converter so as to regulate the output voltage at fixed switching frequency. Its circuit topology is given in Fig. 3. When switch S_2 conducts all the time, the capacitor C_2 is short circuited all the time and the resonant frequency is determined by L and C as $\omega_r = \sqrt{1/(L_r C_r)}$. When the auxiliary switch S_2 does not conduct at all, capacitor C_2 acts as an element of the resonant circuit together with L_r and C_r. The corresponding resonant frequency is $\omega_r = \sqrt{(1/L_r C_r) + (1/L_r C_2)}$. By changing the conduction angle of switch S_2, the equivalent resonant frequency is changed and the output voltage can also be changed. Therefore, the output voltage can be regulated at the constant switching frequency. Unfortunately, at light load, the characteristic of zero voltage switching for S_1 is lost. In addition, the circuit cannot operate at no load condition.

In order to control the class-E dc-to-dc converter at constant switching frequency and also keep zero voltage switching from no load to full load, two identical conventional class-E inverters are combined together with common input and output terminals [12], as shown in Fig. 4, where it is required that $C_1 = C_2$, $L_{r1} = L_{r2}$, $C_{r1} = C_{r2}$ and $L_{f1} = L_{f2}$. The output of

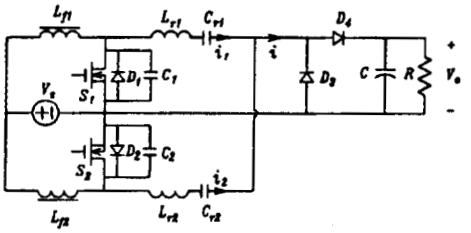

Fig. 4. Class-E combined converter.

these two class-E inverters, i.e., the resonant current i_1 and i_2, are vector added together and then rectified to obtain the dc output. The output voltage is controlled by the phase difference between the drive signals for S_1 and S_2. When the drive signals for S_1 and S_2 are in phase, the current i_1 and i_2 are also in phase and with same amplitude because the two class-E inverters are identical. The output current of the combined converter i is large and the output voltage is high. When the drive signals for S_1 and S_2 are out of phase, i_1 and i_2 are also out of phase and with same amplitude because of symmetry. The output current i is equal to zero, so that the output voltage is zero. By changing the phase shift between the drive signals for S_1 and S_2, the phase angle between i_1 and i_2 and the amplitude of i_1 and i_2 are also changed so that the output voltage is regulated. Using this technique, the output voltage can be regulated at fixed switching frequency and the desirable zero voltage switching for both switches can be maintained from full load to no load. The problem of this scheme is twofold. One is that there are too many components, two input dc choke inductors, two resonant branches. The other is that two resonant branches $L_{r1} - C_{r1}$ and $L_{r2} - C_{r2}$ should be identical and the capacitor in parallel with the two switches C_1 and C_2 should also be identical to ensure symmetrical operation of the converter. This is very difficult in the practical circuit because it is very difficult to control the parasitic parameters which are utilized in the high frequency operation.

From the above analysis, it is, therefore, worthwhile to investigate new class-E dc-to-dc converter topologies that can keep the advantages of the conventional class-E dc-to-dc converter, mainly low switching loss, and at the same time, eliminate its drawbacks, i.e., variable switching frequency control and limited load variation range for lossless operation. The new topology should also be simple. This is really the objective of this work.

III. PROPOSED CLASS-E DC-TO-DC CONVERTER WITH HALF-WAVE CONTROLLED CURRENT RECTIFIER

Let us take a close look at the class-E dc-to-dc converter, as shown in Fig. 1. The output voltage is obtained by rectifying the resonant current i. For the positive half cycle of this current, diode D_3 conducts

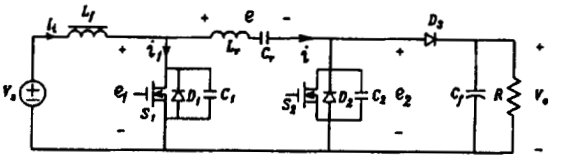

Fig. 5. Proposed class-E converter with half-wave controlled current rectifier.

and the energy is transferred from the resonant branch to the load. For the negative half cycle, diode D_2 conducts and no energy is transferred to the load. When the switching frequency or the equivalent resonant frequency changes, the amplitude of the output current i changes so that the energy delivered to the load changes and consequently, the output voltage changes.

There is another method to regulate the energy delivered to the load resistor. Instead of putting an uncontrolled current rectifier (D_2 and D_3) at the output of class-E inverter, a controlled current rectifier can be used to control the average current delivered to the load resistor, as shown in Fig. 5, where S_2, D_2, C_2, and D_3 consist of the half-wave controlled current rectifier. As compared with the conventional class-E dc-to-dc converter, switch S_2 is introduced to control the energy delivered to the load resistor and capacitor C_2 is used to ensure zero voltage switching of S_2. All the other parts of the converter are the same. In the practical circuit, S_2 and D_2 are composed of a MOSFET and its intrinsic diode, and C_2 is partly composed of its parasitic capacitor, C_{ds}.

The basic idea of this circuit was proposed in our earlier paper in 1992 [13], but the detailed operation principle and the steady state characteristics were not presented.

A similar topology was also presented later in 1993 in [14]. However, the paper did not discuss the various aspects of the topology and the analysis in that paper was not complete.

In the present paper, the proposed class-E dc-to-dc converter has been thoroughly investigated. The operating principle is explained and the mechanism of zero voltage switching for all the switches is outlined. The steady state characteristics are also analyzed and the effects of various parameters are discussed. Some extensions of the proposed circuit are also proposed. Computer simulation by PSPICE and experimental results are provided to verify the feasibility of the circuit and the validity of the analysis.

Assumptions

The operation of the class-E dc-to-dc converter with half-wave controlled current rectifier can be explained as follows. Assume the following.

1) The filter inductor L_f and filter capacitor C_f are large enough so that the input current I_i and output voltage V_0 are pure dc.

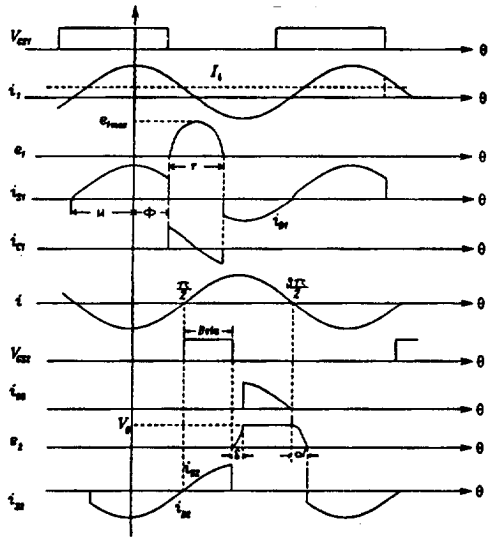

Fig. 6. Typical waveform of Fig. 5.

2) The switches are ideal ones with no transient time and no loss.

3) The losses in the circuit are neglected.

4) The resonant branch, $L_r - C_r$, is a high Q series tuned network. The harmonics of the resonant current i is negligible.

5) The circuit operates at lossless mode, i.e., zero voltage switching for S_1 is maintained.

Notations

Typical waveforms are plotted in Fig. 6. The notations used in the figure are explained as follows:

i_1 is the sum of current flowing through S_1, D_1, and C_1,

e_1 is the voltage across the inverter switch S_1,

γ is the off interval of S_1,

ϕ is the turn off instant of S_1,

$-\mu$ is the turn on instant of S_1,

β is the conduction angle of the rectifier switch and is the control variable,

e_2 is the voltage across the rectifier switch S_2,

i_{C1} is the current flowing through C_1.

The inverter switch S_1 operates at 50% duty ratio. The gate drive signal of the rectifier switch S_2 is synchronized with the resonant current i. S_2 is turned on when the resonant current changes polarity from negative to positive. Just before the resonant current changes direction, it flows through diode D_2. The equivalent circuit is shown in Fig. 7(a). The current direction shown in the figure denotes the actual one. The gate signal for S_2 can be supplied at this time. When the resonant current changes from negative to positive at $\theta = \pi/2$, S_2 conducts and the current flows through S_2, as shown in Fig. 7(b). Therefore, zero voltage turn on for S_2 can always be achieved as the current always commutates from D_2 to S_2. S_2 is turned

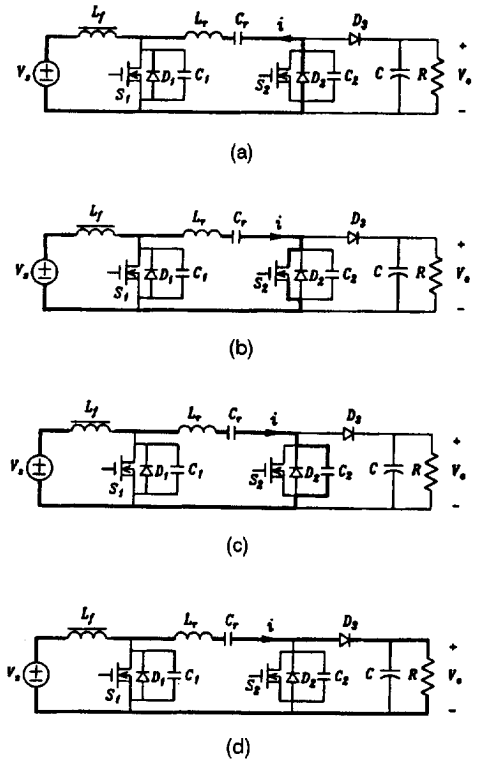

Fig. 7. Path of current flow for half-wave controlled current rectifier. (a) D_2 conducting. (b) S_2 conducting. (c) C_2 charging. (d) D_3 conducting.

off after it conducts for a certain conduction angle, β (the control variable), defined as:

$$\beta = \frac{T_{\text{on}}}{T_s} \cdot 360^\circ \tag{2}$$

where T_s is the switching period, T_{on} is the on time of switch S_2. After S_2 is turned off at $\theta = \pi/2 + \beta$, the resonant current at first charges the capacitor C_2, as shown in Fig. 7(c), and V_{C2} rises slowly. Zero voltage turn off for S_2 is thus obtained. At $\theta = \pi/2 + \beta + \delta$, $V_{C2} = V_0$, diode D_3 is forward biased and the power is delivered from the resonant tank to the load. The equivalent circuit is shown in Fig. 7(d).

The regulation of the output voltage can be described as follows.

1) When $\beta = 0$, which means that the rectifier switch S_2 does not conduct at all, the diode D_3 conducts for the whole positive half cycle of i. The circuit behaves equivalently as the conventional class-E converter. Theoutput voltage is high.

2) When $\beta = 180^\circ$, which means that the rectifier switch S_2 conducts for half switching cycle, all the positive half cycle of the resonant current i flows through S_2. The negative portion of i will flow through diode D_2. The output of the inverter stage is equivalently short circuited. The diode D_3 will never conduct and the output voltage is zero.

3) When the conduction angle β is between 0 and 180°, part of the positive resonant current i

flows through S_2 and part of i flows through D_3. The averaged current through diode D_3 is somewhere between zero and the value corresponding to $\beta = 0$.

When the conduction angle β is varied, the average current through diode D_3, i.e., the output current, is changed and the output voltage will also be changed. Therefore, the output voltage of the converter can be regulated at a fixed switching frequency by modulating the conduction angle β of the rectifier switch S_2.

Another advantage of the class-E converter with controlled current rectifier, given in Fig. 5, is that zero voltage switching for all the switches can be maintained from full load to no load. It is already shown that zero voltage switching for the rectifier switch S_2 can be maintained for entire load range. The following analysis shows that zero voltage switching for the inverter switch S_1 can also be maintained from no load to full load. In the analysis, it is assumed that the steady state output voltage remains constant when load resistor changes.

When the load resistor is small, the conduction angle β should also be kept small so that the conduction angle of diode D_3 is large to provide higher output current. In this case, the equivalent load to the class-E inverter satisfies the lossless operation condition, i.e., see (1). When the load resistor increases, the output current reduces because the output voltage is kept constant. The diode D_3 conducts for shorter period of time and the conduction angle for S_2 is thus increased. The equivalent load appearing at the output of the inverter stage will not increase, but it will actually be reduced. In the extreme case, when the output is open circuit and the load current is zero, S_2 conducts for the whole positive half cycle of i. The inverter output is actually short circuited. Therefore, when the load resistor changes from its minimum to maximum (open circuit), the equivalent resistor appeared at the inverter output reduces from its maximum to zero and (1) is always satisfied. Therefore, zero voltage switching can always be maintained for the inverter switch S_1.

It is shown from the above analysis that the proposed class-E dc-to-dc converter with half-wave controlled current rectifier can keep the switching frequency constant and at the same time keep the desirable zero voltage switching characteristics from no load to full load.

IV. STEADY STATE ANALYSIS

In order to investigate the characteristics of the proposed class-E converter with half-wave controlled current rectifier, the steady state characteristics is analyzed in this section. For simplicity, the Fourier Series Expansion method is used and only the dc and fundamental components are considered. From the waveforms of Fig. 6, the notation and assumptions described in the previous section, the resonant current i can be expressed as:

$$i = -I_p \cos\theta \tag{3}$$

where I_p is the peak value of the resonant current.

From Kirchhoff's current law and from Fig. 5 and (3), we have

$$i_1 = I_i - i = I_i + I_p \cos\theta. \tag{4}$$

The voltage across the inverter switch S_1 can, therefore, be calculated as:

$$e_1 = \begin{cases} \frac{1}{\omega_s C_1}\int_{\phi}^{\theta} i_1\, d\theta = \frac{1}{\omega_s C_1}[I_i(\theta-\phi) + I_p(\sin\theta - \sin\phi)] \\ \qquad\qquad \text{for} \quad \phi \le \theta \le \phi + \gamma \\ 0 \qquad\qquad \text{elsewhere.} \end{cases} \tag{5}$$

For lossless operation we have

$$e_1(\theta = \phi + \gamma) = 0. \tag{6}$$

From (5) and (6), the following equation is obtained:

$$\gamma I_i = I_p[\sin\phi - \sin(\phi + \gamma)]. \tag{7}$$

Expanding the voltage e_1 into Fourier series and only considering the dc and fundamental components, the following equation is obtained:

$$e_1 = E_1 + E_{11}\cos\theta + E_{12}\sin\theta \tag{8}$$

where

$$E_1 = \frac{I_p}{2\pi\omega_s C_1}\left[\frac{I_i}{I_p}\frac{\gamma^2}{2} - \cos(\phi+\gamma) + \cos\phi - \gamma\sin\phi\right] \tag{9}$$

$$E_{11} = \frac{I_p}{\pi\omega_s C_1}\left\{\frac{I_i}{I_p}[\gamma\sin(\phi+\gamma) + \cos(\phi+\gamma) - \cos\phi] - \tfrac{1}{4}\cos 2(\phi+\gamma) - \sin\phi\sin(\phi+\gamma) - \tfrac{1}{4}\cos 2\phi + \tfrac{1}{2}\right\} \tag{10}$$

$$E_{12} = \frac{I_p}{\pi\omega_s C_1}\left\{\frac{I_i}{I_p}[-\gamma\cos(\phi+\gamma) + \sin(\phi+\gamma) - \sin\phi] - \tfrac{1}{4}\sin 2(\phi+\gamma) + \sin\phi\cos(\phi+\gamma) - \tfrac{1}{4}\sin 2\phi + \frac{\gamma}{2}\right\}. \tag{11}$$

Because the voltage across the input inductor has no dc component, the average voltage across S_1 is the same as the supply voltage, i.e.,

$$V_s = E_1 = \frac{I_p}{2\pi\omega_s C_1} \times \left[\frac{I_i}{I_p}\frac{\gamma^2}{2} - \cos(\phi+\gamma) + \cos\phi - \gamma\sin\phi\right]. \tag{12}$$

According to the waveforms shown in Fig. 6, at $\theta = \pi/2 + \beta$, the rectifier switch S_2 is turned off. The capacitor C_2 is charged by the resonant current i and the voltage e_2 rises. At $\theta = \pi/2 + \beta + \delta$, e_2 reaches V_0 and D_3 is turned on. The voltage e_2 is clamped at V_0 by D_3, as shown in Fig. 6. At $\theta = 3\pi/2$, the capacitor C_2 is discharged by the negative part of the resonant current and e_2 falls to zero. The expression for e_2 can be found as:

$$e_2 = \begin{cases} \dfrac{I_p}{\omega_s C_2}(\cos\beta - \sin\theta) & \dfrac{\pi}{2} + \beta \le \theta \le \dfrac{\pi}{2} + \beta + \delta \\ V_0 & \dfrac{\pi}{2} + \beta + \delta \le \theta \le \dfrac{3\pi}{2} \\ V_0 - \dfrac{I_p}{\omega_s C_2}(1 + \sin\theta) & \dfrac{3\pi}{2} \le \theta \le \dfrac{3\pi}{2} + \alpha \\ 0 & \text{elsewhere} \end{cases} \tag{13}$$

where δ and α are expressed as:

$$\delta = \cos^{-1}\left(\cos\beta - \frac{V_0\omega_s C_2}{I_p}\right) - \beta,$$
$$\alpha = \cos^{-1}\left(1 - \frac{V_0\omega_s C_2}{I_p}\right). \tag{14}$$

The Fourier expansion of e_2 can be expressed as:

$$e_2 = E_2 + E_{21}\cos\theta + E_{22}\sin\theta \tag{15}$$

where the high-order harmonics are neglected. E_{21} and E_{22} are expressed as:

$$E_{21} = \frac{I_p}{4\pi\omega_s C_2}\{4\cos\beta[\cos(\beta+\delta) - \cos\beta] + \cos 2\beta - \cos 2(\beta+\delta) - (1 - \cos 2\alpha)\} - \frac{1}{\pi}V_0[1 + \cos(\beta+\delta)] + \frac{1}{\pi}\left(V_0 - \frac{I_p}{\omega_s C_2}\right)(1 - \cos\alpha) \tag{16}$$

$$E_{22} = \frac{I_p}{4\pi\omega_s C_2}\{4\cos\beta[\sin(\beta+\delta) - \sin\beta] - \sin 2(\beta+\delta) + \sin 2\beta - \sin 2\alpha - 2(\delta+\alpha)\} - \frac{1}{\pi}V_0\sin(\beta+\delta) - \frac{1}{\pi}\left(V_0 - \frac{I_p}{\omega_s C_2}\right)\sin\alpha. \tag{17}$$

The voltage across the resonant branch, $L_r - C_r$, is found as:

$$e = E + I_p\left(\omega_s L_r - \frac{1}{\omega_s C_r}\right)\sin\theta. \tag{18}$$

From Kirchhoff's voltage law, the following equation for the fundamental component is derived:

$$E_{11}\cos\theta + E_{12}\sin\theta = I_p\left(\omega_s L_r - \frac{1}{\omega_s C_r}\right)\sin\theta + E_{21}\cos\theta + E_{22}\sin\theta. \tag{19}$$

Two equations can be derived from (20) as:

$$E_{11} = E_{21} \tag{20}$$

$$E_{12} = I_p\left(\omega_s L_r - \frac{1}{\omega_s C_r}\right) + E_{22} \tag{21}$$

where the expressions for E_{11}, E_{12} and E_{21}, E_{22} can be found in (10), (11), (16), and (17). In the analysis, the load resistor R, supply voltage V_s, and the desired output voltage V_0 are known. Therefore, the input current I_i can be calculated from the power balance as:

$$I_i = \frac{V_0^2}{RV_s}. \tag{22}$$

There are four unknowns, I_p, β, ϕ, and γ in four equations (7), (12), (20) and (21). Given the supply voltage V_s, load resistor R and the desired output voltage V_0, as well as the circuit variables, L_r, C_r, C_1, C_2, the required conduction angle β, I_p, ϕ, and γ can all be obtained.

The voltage stress for inverter switch S_1 can be obtained from (5) by setting $de_1/d\theta = 0$ and calculated as:

$$e_{1\max} = \frac{1}{\omega_s C_1}[I_i(\theta_m - \phi) + I_p(\sin\theta_m - \sin\phi)] \tag{23}$$

where θ_m is expressed as: $\theta_m = \cos^{-1}(I_i/I_p)$.

The peak voltage across the rectifier switch is the output voltage, i.e.,

$$e_{2\max} = V_0. \tag{24}$$

The rms value of the current flowing through S_1 is calculated as follows:

$$I_{1\text{rms}} = \sqrt{\frac{1}{2\pi}\int_{-\mu}^{\phi}(I_i + I_p\cos\theta)^2 d\theta} = \sqrt{\frac{1}{2\pi}\left[I_i^2(\phi+\mu) + 2I_iI_p(\sin\phi + \sin\mu) + I_P^2\left(\frac{\phi+\mu}{2} - \frac{\sin 2\phi - \sin 2\mu}{4}\right)\right]} \tag{25}$$

where μ is calculated from $\mu = \cos^{-1}(-I_i/I_p)$.

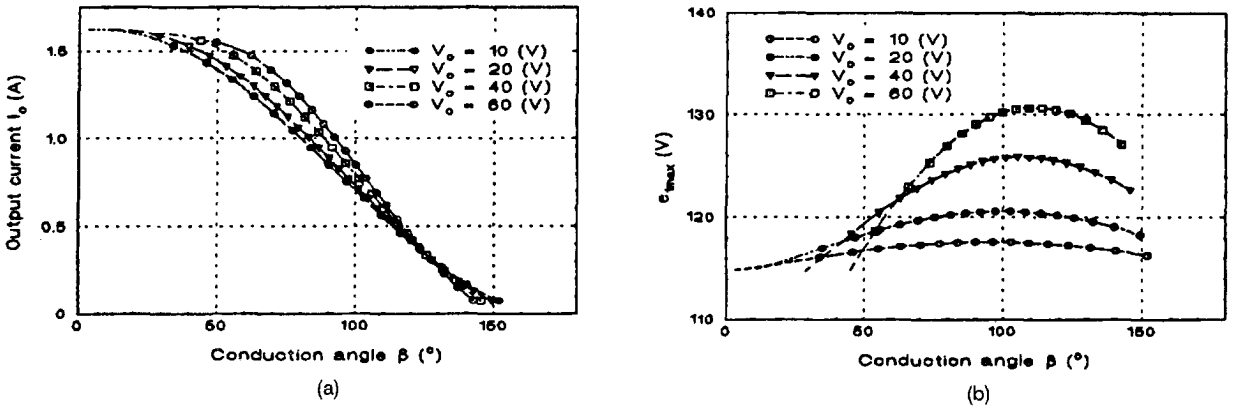

Fig. 8. Effect of output voltage on (a) load current I_0 and (b) voltage stress of S_1 at $V_s = 30$ V, $C_1 = 5$ nF, $C_2 = 2.5$ nF, $X = 10\ \Omega$, $f_r = 0.9$ MHz, $f_s = 1$ MHz.

The rms value of the current flowing through S_2 is

$$I_{2\max} = \sqrt{\frac{1}{2\pi}\int_{\pi/2}^{\pi/2+\beta} (-I_p\cos\theta)^2\, d\theta}$$

$$= I_p\sqrt{\frac{1}{2\pi}\left(\frac{\beta}{2} - \frac{\sin 2\beta}{4}\right)}. \tag{26}$$

Based on the above equations, the characteristics of the class-E dc-to-dc converter with half-wave controlled current rectifier can be analyzed. In the analysis, the parameters for the resonant branch, L_r and C_r, are defined as the resonant frequency $f_r (f_r = \sqrt{1/(2\pi L_r C_r)})$ and the branch impedance $X (X = \omega_s L_r - (1/\omega_s C_r))$. The L_r and C_r can be calculated easily from f_r and X as:

$$L_r = \frac{X}{2\pi f_s\left[1 - \dfrac{(2\pi f_r)^2}{(2\pi f_s)^2}\right]}$$

$$C_r = \frac{1}{(2\pi f_r)^2 L_r}. \tag{27}$$

At first the effect of the desired output voltage is examined. Fig. 8(a) gives the relationship between the output current and the control input (the conduction angle β) for different output voltage, $V_0 = 10$ V, 20 V, 40 V, and 60 V. The circuit parameters are: $V_s = 30$ V, $C_1 = 5$ nF, $C_2 = 2.5$ nF, $X = 10\ \Omega$, $f_r = 0.9$ MHz and $f_s = 1$ MHz. It shows that the output voltage can be kept at the desired value by changing the conduction angle β when the load current I_0 changes. The effect of the output voltage on the output current is not very large, e.g., when the output voltage changes from 10 V to 60 V at $\beta = 50°$, the corresponding output current changes only from about 1.35 A to about 1.55 A. It is also noticed that the curves do not go down to $\beta = 0$. This is because the output of the class-E inverter can only be considered as weak current source. It cannot provide high enough current to keep the output voltage constant (as the output voltage is assumed constant in the above analysis) when the load resistor becomes too small. In the analysis, this fact is shown as no real solution for smaller β. It is also noted that the conduction angle β will never reach 180° because of the charging time for C_2. The largest possible β depends on the value of C_2 and amplitude of i. It also depends on the value of the output voltage V_0. When V_0 is high, the time used to charge C_2 is longer and the largest possible β is less and vice versa.

The effect of theoutput voltage on the voltage stress of the inverter switch S_1, $e_{1\max}$, is also analyzed, as shown in Fig. 8(b). It shows that when the desired output voltage becomes higher, the voltage stress also becomes higher. But again, the influence is not very significant, i.e., when the desired output voltage increases from 10 V to 60 V, the maximum voltage across S_1 increases from about 115 V to about 130 V. The other observation is that for a certain output voltage, the voltage stress will increase a little bit (about 14% for $V_0 = 60$ V and about 2% for $V_0 = 10$ V) when the conduction angle β increases. It is noted that when C_2 is charged up, the resonant frequency is changed due to the presence of C_2. Therefore, $e_{1\max}$ is different which is similar to the case of conventional class-E converter at different switching frequency. At high output voltage, the time needed to charge C_2 is longer. Therefore, the effect of C_2 on the resonant frequency is larger and $e_{1\max}$ varies more as compared with a low output voltage case, as can be seen from Fig. 8(b).

The effect of the impedance of the resonant branch X is also studied. The circuit parameters in the analysis are: $V_s = 30$ V, $V_0 = 30$ V, $C_1 = 5$ nF, $C_2 = 2.5$ nF, $f_r = 0.9$ MHz, $f_s = 1$ MHz. The effect of X on the output current is given in Fig. 9(a). It shows that the output current increases when X reduces. This phenomenon is understandable because for smaller X, the amplitude of the resonant current increases and therefore, the output current also increases. The voltage stress for S_1 also increases when the impedance of the resonant branch reduces, as shown in Fig. 9(b).

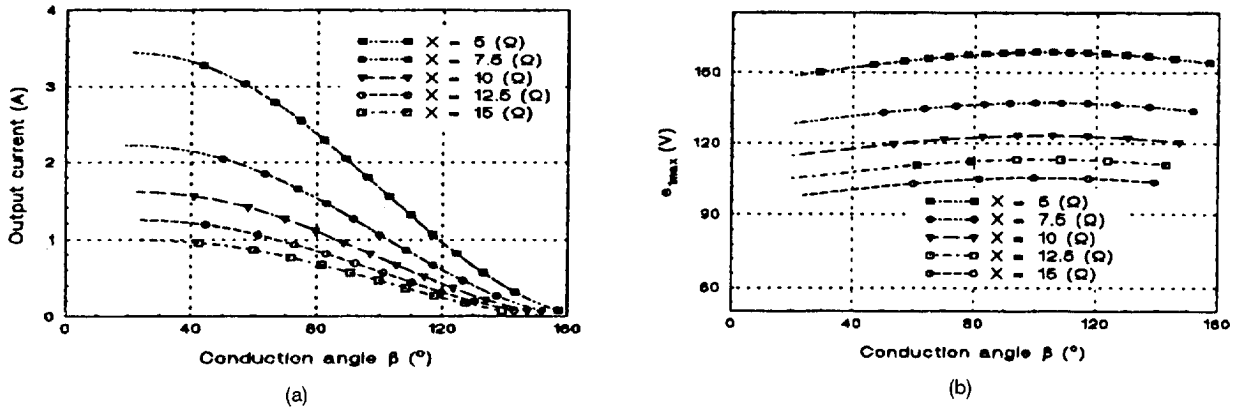

Fig. 9. Effect of resonant impedance on (a) output current and (b) voltage stress of S_1 at $V_s = 30$ V, $V_0 = 30$ V, $C_1 = 5$ nF, $C_2 = 2.5$ nF, $f_r = 0.9$ MHz, $f_s = 1$ MHz.

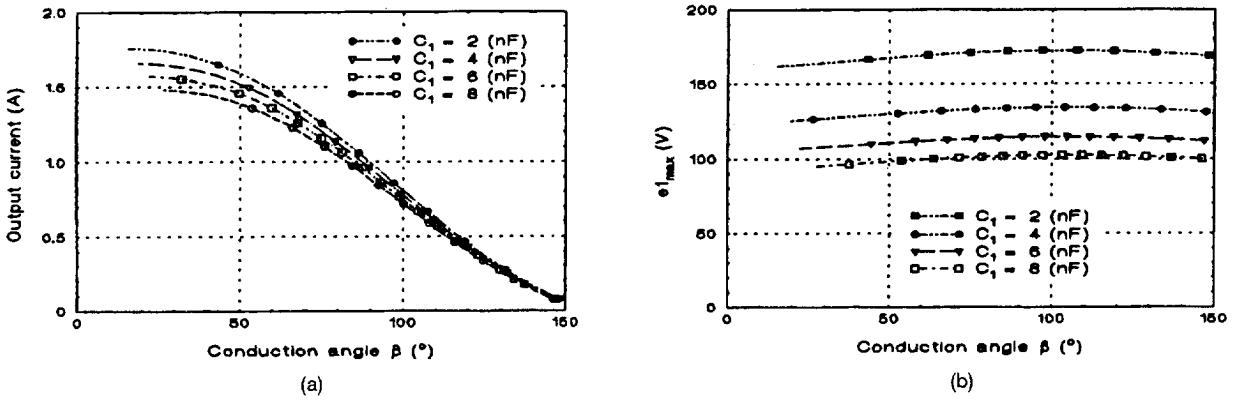

Fig. 10. Effect of parallel capacitor C_1 on (a) output current and (b) voltage stress of S_1 at $V_s = 30$ V, $V_0 = 30$ V, $C_2 = 2.5$ nF, $X = 10\ \Omega$, $f_r = 0.9$ MHz, $f_s = 1$ MHz.

The effect of the capacitor in parallel with the inverter switch S_1 is also analyzed with the circuit parameter: $V_s = 30$ V, $V_0 = 30$ V, $C_2 = 2.5$ nF, $X = 10\ \Omega$, $f_r = 0.9$ MHz, $f_s = 1$ MHz. The results are plotted in Fig. 10. It is shown that when C_1 increases, the voltage stress on S_1 is reduced significantly, as given in Fig. 10(b). On the other hand, the effect of C_1 on the output current is not significant, as shown in Fig. 10(a). This is a good feature, which illustrates that in the class-E dc-to-dc converter with half-wave controlled current rectifier, the voltage stress of S_1 can be reduced by a larger C_1 while the output current is not sacrificed.

Similarly, the effect of other circuit parameters can also be analyzed. The effect of the capacitor in parallel with the rectifier switch C_2 is not significant and the resonant frequency f_r has no effect on the output current, but f_r will affect the voltage across C_r and L_r. The details are not presented here.

V. SOME EXTENSIONS OF THE PROPOSED CIRCUIT

When the half-wave controlled current rectifier used in Fig. 5 is replaced by a full-wave controlled current rectifier, the class-E dc-to-dc converter with full-wave controlled current rectifier is obtained, as shown in Fig. 11, where the inverter stage is the same as that in Fig. 5. The full-wave controlled current rectifier is composed of $S_2D_2C_2$, $S_3D_3C_3$, and D_4, D_5.

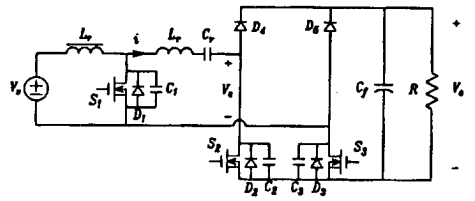

Fig. 11. Class-E dc-to-dc converter with full-wave controlled current rectifier.

The control signal is arranged as follows. The gate drives for S_2 and S_3 are synchronized with the resonant current i. S_2 is turned on when i changes polarity from negative to positive and conducts for conduction angle β. S_3 is turned on when i changes from positive to negative and also conducts for the conduction angle β. By changing the conduction angle β, the output voltage can be regulated in the similar manner as that of half-wave controlled current rectifier. For example, when S_2 and S_3 does not conduct at all, the circuit

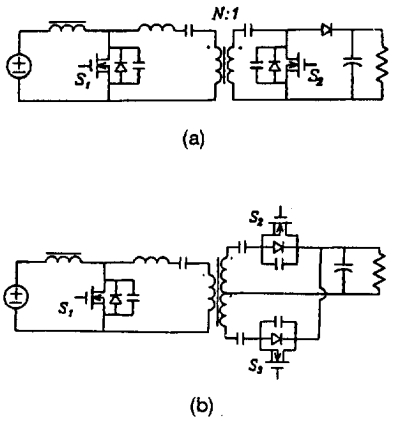

Fig. 12. Isolated version of class-E dc-to-dc converters with controlled current rectifier. (a) Half-wave. (b) Full-wave.

behaves like the conventional class-E converter with full-wave rectifier and the output voltage is high. When S_2 and S_3 conduct as long as they can, the output voltage is zero.

Zero voltage switching for S_2 and S_3 can always be maintained from no load to full load as the parallel capacitors C_2 and C_3 can always be discharged by the resonant current i and this is independent of the load current. The switching condition for the inverter switch S_1 is similar to the half-wave controlled current rectifier and zero voltage switching can also be maintained from no load to full load.

When the isolation between the input side and the output side is necessary or large voltage gain is required, an isolation transformer can be added for both the half-wave and full-wave controlled current rectifier, as shown in Fig. 12. Fig. 12(a) is the half-wave version and Fig. 12(b) is the full-wave one. Their operating principle is similar to that of nonisolated ones and are not explained here. The capacitors at the secondary side of the transformers in Fig. 12(a) and Fig. 12(b) are used to block the dc component to avoid saturation of the transformer.

VI. COMPUTER SIMULATION AND EXPERIMENTAL VERIFICATION

The operation of the class-E dc-to-dc converter with half-wave controlled current rectifier (Fig. 5)

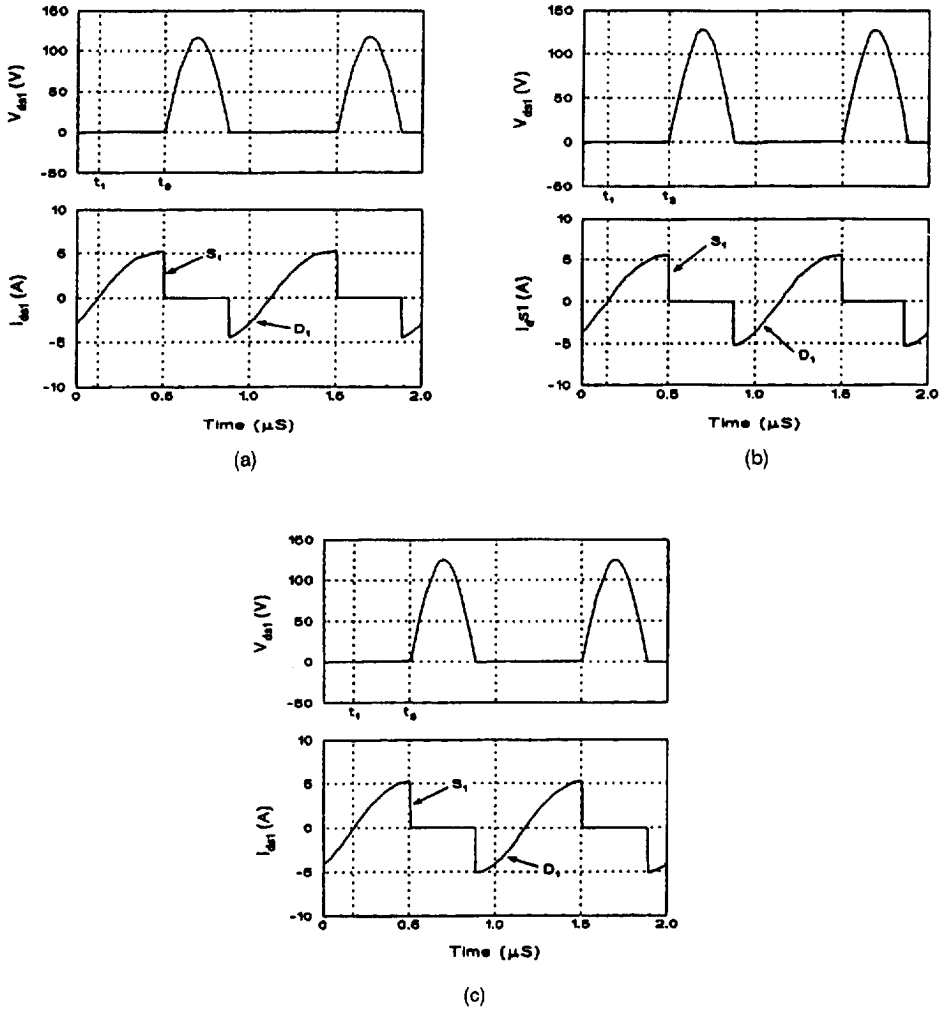

Fig. 13. Switching waveforms at S_1 at different conduction angle β. (a) $\beta = 0°$. (b) $\beta = 90°$. (c) $\beta = 144°$.

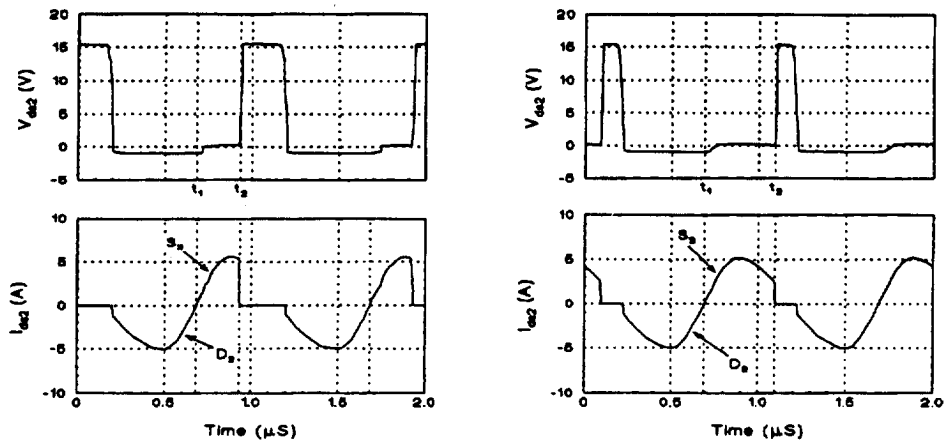

(a) (b)

Fig. 14. Switching waveforms of S_2 at different conduction angle β. (a) $\beta = 90°$. (b) $\beta = 144°$.

is simulated by PSPICE to show the feasibility of the proposed circuit. The circuit parameters used in the simulation are: $L_r = 4.5\ \mu$H, $C_r = 9$ nF, $C_1 = 5$ nF, $C_2 = 1.5$ nF, and $L_f = 100\ \mu$H. The switching frequency is selected as 1 MHz. The supply voltage $V_s = 30$ V and the output is modeled by a constant voltage source with $V_0 = 15$ V.

Figs. 13 and 14 give the switching waveforms of S_1 and S_2 for the class-E converter with half-wave controlled current rectifier. Fig. 13 gives the voltage V_{ds1} and current I_{ds1} associated with the inverter switch S_1 at different conduction angle, β, (a) $\beta = 0$, i.e., S_2 does not conduct at all, which is equivalent to the conventional class-E converter, (b) $\beta = 90°$ when S_2 conducts for half of the positive cycle of the resonant current i, and (c) $\beta = 144°$ when the output current is very small. It is shown that when the current commutates from the antiparallel diode to S_1 (at t_1 in Fig. 13), the voltage across S_1 is zero. Zero voltage turn on is achieved. When S_1 is turned off at t_2, as shown in Fig. 13, the voltage V_{ds1} rises slowly. Zero voltage switching for S_1 can be observed for all these operating conditions. Fig. 14 gives the switching waveforms of the rectifier switch S_2 when (a) $\beta = 90°$ and (b) $\beta = 144°$, respectively. It is also illustrated that when S_2 is turned on (at time t_1), the voltage across it is zero and when S_2 is turned off, the voltage v_{ds2} rises slowly (at time t_2 in Fig. 14). Obviously, zero voltage switching is achieved.

An experimental prototype of class-E dc-to-dc converter with half-wave controlled current rectifier is also breadboarded in order to show the feasibility of the proposed circuit and the validity of the analysis. The experimental circuit is the same as that shown in Fig. 5. The circuit parameters used in the experiment are as follows: $V_s = 30$ V, $L_r = 4.4\ \mu$H, $C_r = 9$ nF, $C_1 = 5.5$ nF, $C_2 = 2.3$ nF, $L_f = 106\ \mu$H, $C = 52\ \mu$F. The switching frequency is fixed at 1 MHz and the output voltage is regulated at 15 V. The load resistor changes from 10 Ω to open circuit.

Fig. 15 gives the gate drive signal and device voltage of the inverter switch S_1 at different conduction angle β. Fig. 15(a) gives the waveforms when $\beta = 44°$ and the output current is measured as 1.46 A. Fig. 15(b) is the waveforms when $\beta = 82°$ and the output current is at 0.9 A. Fig. 15(c) shows the waveforms when the output current is zero and $\beta = 144°$. It is observed from these oscillograms that when the gate signal V_{GS1} rises to 15 V (device turn on), the voltage across S_1, V_{DS1}, is zero and when the gate signal V_{GS1} falls to zero (device turn off), the voltage V_{DS1} rises slowly. Therefore, zero voltage switching for the inverter switch S_1 can be maintained for the entire output current range.

Fig. 16 gives the gate signal and the device voltage of the rectifier switch S_2 for different conduction angle β. Fig. 16(a) and Fig. 16(b) give the waveform when $\beta = 60°$ and $\beta = 144°$, respectively. When $\beta = 144°$, the output current is zero. It can also be observed that when the gate signal for S_2 (i.e., V_{GS2}), rises to 15 V, the voltage across S_2 (i.e., V_{DS2}), is zero and when the gate signal V_{GS2} falls to zero, the voltage V_{DS2} rises from zero value. This shows that zero voltage switching is achieved for the rectifier switch S_2.

The relation between the steady state output current versus the conduction angle β is also measured when the output voltage is regulated at 15 V, as shown in Fig. 17. The calculated value is also plotted at the same graph. These two curves are very close. The small difference is caused by the nonideality of the prototype. It demonstrates that by changing the conduction angle of the rectifier switch, the output voltage can be kept at the desired value when the output current changes.

VII. CONCLUSION

In this paper, the present techniques of the class-E dc-to-dc converters are reviewed and their drawbacks

(a)

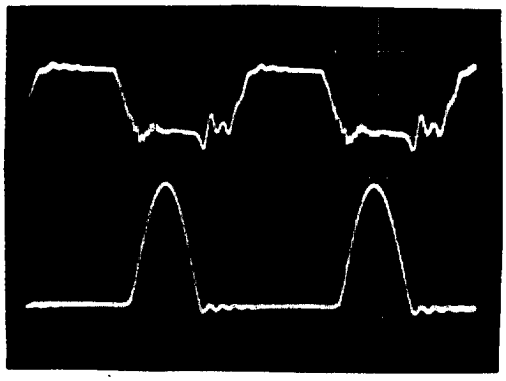

(b)

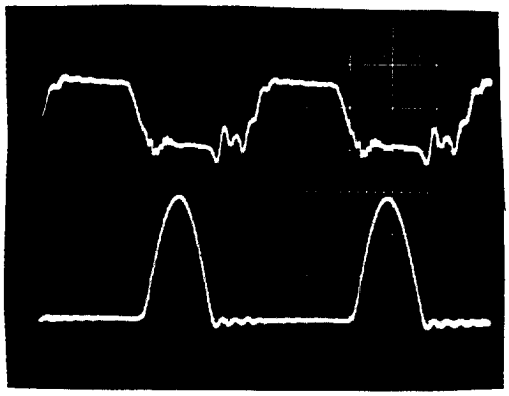

(c)

Fig. 15. Switching waveforms of inverter switch S_1 at (a) $\beta = 44°$, (b) $\beta = 82°$, (c) $\beta = 144°$. Upper trace: V_{GS1}, 10 V/div, lower trace: V_{DS1}, 50 V/div. Horizontal: 0.2 μS/div.

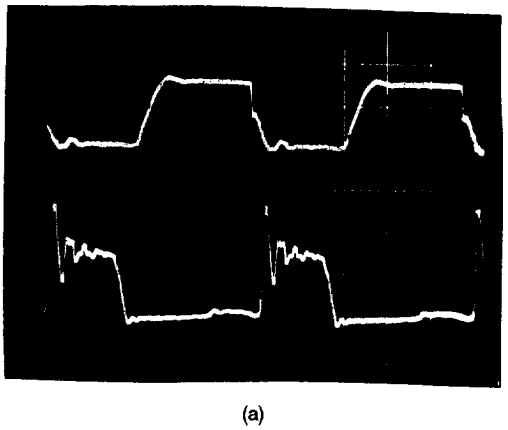

(a)

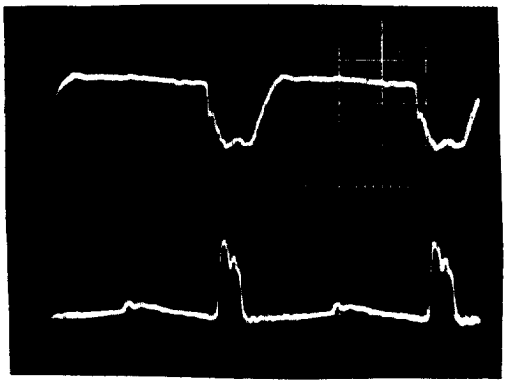

(b)

Fig. 16. Switching waveforms of rectifier switch S_2 at (a) $\beta = 60°$ and (b) $\beta = 144°$. Upper trace: V_{GS2}, 10 V/div, lower trace: V_{DS2}, 10 V/div. Horizontal: 0.2 μS/div.

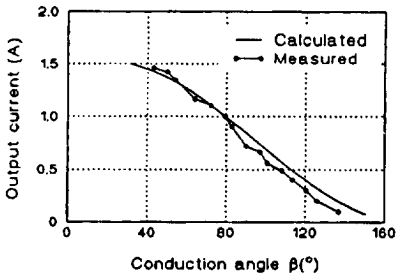

Fig. 17. Calculated and measured output current.

are addressed. A new class-E dc-to-dc converter topology with half-wave controlled current rectifier is proposed. The mechanism to maintain the zero voltage switching for all the switches is explained. The output voltage can be regulated by changing the conduction angle of the rectifier switch. The salient advantages of the new converter topologies are: 1) the switching frequency is constant, 2) the circuits can operate at no load condition, and 3) zero voltage switching for all the switches can be maintained from no load to full load.

The steady state characteristics of the proposed class-E dc-to-dc converter with half-wave controlled current rectifier is analyzed. The effects of the circuit parameters on the output current are also studied. The analysis shows that the output current can be regulated by the conduction angle of the rectifier switch to keep the output voltage constant. Some extensions of the proposed circuit, i.e., class-E dc-to-dc converter with full-wave controlled current rectifier, the isolated

class-E converters with controlled current rectifier, are also presented.

The operation of the class-E dc-to-dc converter with half-wave controlled current rectifier is simulated by PSPICE to show the feasibility of the proposed circuit. An experimental prototype is also breadboarded to demonstrate the feasibility of the proposed class-E converter and to verify the analysis. Zero voltage switching is shown clearly in the simulation and the experimental oscillograms. The measured relation between output current and conduction angle is very close to the calculated one.

REFERENCES

[1] Sen, P. C. (1981)
Thyristor DC Drives.
New York: Wiley, 1981.

[2] Sen, P. C. (1988)
Principles of Electric Machines and Power Electronics.
New York: Wiley, 1988.

[3] Mohan, N., Undeland, T. M., and Robbins, W. P. (1989)
Power Electronics, Converter, Applications and Designs.
New York: Wiley, 1989.

[4] Rashid, M. H. (1988)
Power Electronics, Circuits Devices and Applications.
Englewood Cliffs, NJ: Prentice Hall, 1988.

[5] Steigerwald, R. L. (1984)
High-frequency resonant transistor DC–DC converters.
IEEE Transactions on Industry Electronics, **31** (May 1984), 181–191.

[6] Ranganathan, V. T., Ziogas, P. D., and Stefanovic, V. R. (1982)
A regulated DC–DC voltage source converter using a high-frequency link.
IEEE Transactions on Industrial Applications, **IA-18** (May/June 1982), 279–287.

[7] Steigerwald, R. L. (1988)
A comparison of half-bridge resonant converter topologies.
IEEE Transactions on Power Electronics, **3**, 2 (Apr. 1988), 174–182.

[8] Redl, R., Molnar, B., and Sokal, N. O. (1986)
Class-E resonant DC/DC power converters: Analysis of operations, and experimental results at 1.5 MHz.
IEEE Transactions on Power Electronics, **PE-1**, 2 (Apr. 1986), 111–119.

[9] Lütteke, G., and Raets, H. C. (1987)
220-V mains 500-KHz class-E converter using a BIMOS.
IEEE Transactions on Power Electronics, **2**, 3 (July 1987), 186–193.

[10] Kazimierczuk, M. K., and Bui, X. T. (1989)
Class-E DC/DC converters with an inductive impedance inverter.
IEEE Transactions on Power Electronics, **4**, 1 (Jan. 1989), 124–135.

[11] Gu, W. J., and Harada, K. (1988)
A new method to regulate resonant converters.
IEEE Transactions on Power Electronics, **3**, 4 (1988), 430–439.

[12] Hu, C. Q., Zhang, X. Z., and Huang, S. P. (1989)
Class-E combined converter by phase-shift control.
In *IEEE Power Electronics Specialists Conference Record*, (1989), 229–234.

[13] Liu, Y.-F., and Sen, P. C. (1992)
Source reactance lossless switch (SRLS) for soft-switching converters with constant switching frequency.
In *IEEE Industry Application Society 1992 Annual Meeting Record*, (1992), 710–719.

[14] Mikolajewski, M. (1993)
DC/DC resonant converter with synchronous regulated rectifier.
In *Proceedings of High Frequency Power Conversion Conference*, (1993), 21–35.

Yan-Fei Liu (S'90—M'94) received the B.Sc. and M.Sc. degrees in Department of Electrical Engineering from Zhejiang University, Hangzhou, People's Republic of China in 1984 and 1987, respectively, and Ph.D. degree from Queen's University, Kingston, Canada in 1994.

He was an Assistant Professor at Zhejiang University from 1987 to 1990. From September 1990 to February 1994, he was at Queen's University working toward the Ph.D. degree where he was employed as a research and teaching assistant. He was also employed as an Adjunct Instructor from September 1993 to December 1993. Dr. Liu is currently a Power Supply Designer with the Power Group, Bell Northern Research Ltd., Ottawa, Canada. His research interests include new circuit configurations of soft switching converters, control techniques to improve the dynamic performance of PWM switching converters, and dynamic modeling and computer simulation of switching power converters.

Paresh C. Sen (M'67—SM'74—F'89) was born in Chittagong, Bangladesh. He received the B.Sc. (Hons.) in physics and the M.Sc. (Tech) degree in applied physics from the University of Calcutta, India, in 1958 and 1961, respectively. He received the M.A.Sc. and Ph.D. degrees in Electrical Engineering from the University of Toronto, Ontario, Canada, in 1965 and 1967, respectively.

He is currently Professor of Electrical Engineering at Queen's University, Kingston, Ontario, Canada. His fields of interest are power electronics and drives, microcomputer control of electric drives systems, modern control techniques for high-performance drive systems, and switching power supplies.

Dr. Sen has authored more than 90 research papers in the general area of power electronics and drives. He is the author of two books: *Thyristor DC Drives* (New York: Wiley, 1981) and *Principles of Electric Machines and Power Electronics* (New York: Wiley, 1988).

He served as an Associate Editor for *IEEE Transactions on Industrial Electronics and Control Instrumentation* (IECI 1975–1982) and as Chairman of the Technical Committees (IECI Society) on Power Electronic (1979–1980) and Energy Systems (1980–1982). He has served on program committees of many IEEE and international conferences and has organized and chaired many technical sessions. At present, he is an active member of the Industrial Drives Committee and the Static Power Converter Committee of IEEE Industry Applications Society. He is also a member of the International Steering Committee on International Conference on Electric drives (ICED). He is internationally recognized as a specialist in power electronics and drives. He received a Prize Paper Award from the Industrial Drive Committee for technical excellence at the Industry Applications Society Annual Meeting in 1986.